

Theory of thermal conductivity in extended- s state superconductors: application to ferropnictides

V. Mishra¹, A. Vorontsov², P.J. Hirschfeld¹, and I. Vekhter³

¹Department of Physics, University of Florida, Gainesville, FL 32611, USA

²Department of Physics, Montana State University, Bozeman, MT 59717 USA

³Department of Physics and Astronomy, Louisiana State University, Baton Rouge, LA 70803, USA

(Dated: November 13, 2018)

Within a two-band model for the recently discovered ferropnictide materials, we calculate the thermal conductivity assuming general superconducting states of A_{1g} (“ s -wave”) symmetry, considering both currently popular isotropic “sign-changing” s states and states with strong anisotropy, including those which manifest nodes or deep minima of the order parameter. We consider both intra- and interband disorder scattering effects, and show that in situations where a low-temperature linear- T exists in the thermal conductivity, it is not always “universal” as in d -wave superconductors. We discuss the conditions under which such a term can disappear, as well as how it can be induced by a magnetic field. We compare our results to several recent experiments.

PACS numbers:

I. INTRODUCTION

The symmetry class of the newly discovered ferropnictide superconductors² is still controversial, due in part to differing results on superfluid density^{3,4,5,6,7,8}, angle-resolved photoemission (ARPES)^{9,10,11,12,13,14}, nuclear magnetic resonance (NMR)^{15,16,17,18,19,20}, Andreev spectroscopy^{21,22,23,24}, and other experimental probes. In some cases, these experiments have been interpreted as implying the absence of low-energy excitations, i.e. a fully developed spectral gap. In others, low-energy excitations have been observed, and taken as indication of the existence of order parameter nodes. It may be that these differences depend on the stoichiometry or doping of the materials, which affects the pairing interaction, or sample quality, or both.

As in other classes of potentially unconventional superconductors, one’s ability to identify the symmetry class of a candidate material by observation of low- T power laws in temperature reflecting low energy quasiparticle excitations is limited by how low in T one can measure. At intermediate temperatures, variations of thermodynamic and transport properties can be affected by details of band structure, elastic and inelastic scattering, as well as the presence of thermal phonons. Only at the very lowest T can one – in principle – extract direct information on the order parameter structure. Thermal conductivity measurements have played an important role in past discussions of unconventional superconductivity^{25,26}, in part because they can be extended to T of order tens of mK. In addition, such measurements are distinguished because they are bulk probes, and because they are unusually sensitive to the presence of order parameter nodes. If lines of nodes are present, the thermal conductivity $\kappa(T)$ manifests a low- T linear, in temperature, term which is purely electronic in origin and is associated with residual quasiparticle states at the Fermi level, induced by disorder or a magnetic field. If, in addition, the order parameter averages to zero over the Fermi surface

(as in the d -wave case appropriate for the cuprates), this linear- T term in zero field is known to be “universal”, in the sense that its magnitude is only weakly disorder dependent.

Very recently, several low-temperature measurements of thermal transport have been made on the BaFe_2As_2 (Ba-122) material doped with K ^{27,28}, Co ³⁷ and Ni ²⁹, as well as on the stoichiometric superconductor LaFePO ³¹. In the case of the Ba-122 samples, either zero or very small linear- T terms have been reported in zero field, leading to the conclusion that there is a fully developed spectral gap in these materials³² in these experimental works. This is in contrast to reports of power law temperature dependence in the superfluid density measured on the same materials^{3,4,5,6,7}, as well as other strong indications of low-energy excitations. One way to reconcile these experiments is to note that thermal conductivity at mK temperatures probes lower energy scales than those measured in other experiments to date; thus it is possible that a band of low-energy excitations extends to very low energies, but not all the way to the Fermi level, either due to an intrinsic highly anisotropic order parameter with deep minima, or a band of impurity states which lies at low but nonzero excitation energies. Such impurity states can be produced, e.g., in isotropic, sign-changing s -wave pair state^{33,34,35,36} allowable in multiband systems if special conditions on the ratio of intra- to interband scattering are met. However, a further strong constraint from the thermal conductivity measurements is that a significant linear- T term in the thermal conductivity is observed with the application of a small magnetic field of order one Tesla and hence much below the upper critical field, H_{c2} . This residual term grows with increasing field. This would be consistent with the existence of quasiparticle states at low, but finite energy. Refs. 28,37 on K- and Co-doped Ba-122 samples claimed that this enhancement is significantly larger than that to be expected in the case of a conventional s -wave superconductor. In contrast, Ref. 29 came to opposite conclusions

on the measurements of a Ni-doped sample, and Ref. 30 reported a small but significant linear- T term in zero field in Co-doped Ba-122.

A recent measurement of $\kappa(T)$ on the ferrophosphide superconductor LaFePO finds a very large linear- T term³¹. If this is interpreted as indicative of order parameter nodes, it would be consistent with the linear- T dependence in the superfluid density also observed for this system⁸. Note that disorder in a sign-changing s state cannot produce such a term in the superfluid density. This material is the only material yet discovered among the growing ferropnictide family of superconductors whose undoped “parent compound” is superconducting at zero pressure. It is therefore expected to be significantly cleaner than other superconductors discussed here. This may be relevant because it has been proposed that disorder in highly anisotropic “s-wave” (A_{1g} symmetry) states can “lift” shallow nodes in the order parameter, leading to a fully developed spectral gap³⁸. The authors of Ref. 31 note that, despite a very sharp resistive transition, they cannot completely exclude the possibility that the linear- T term is partly extrinsic; however, even in that case the dominant dependence of the thermal conductivity on the magnetic field should come from the superconducting phase.

There is a developing consensus that the gap changes sign between the electron and hole Fermi surface sheets. From the theoretical standpoint, states with nodes or deep minima appear to be quite natural. Several microscopic theories of the spin fluctuation mediated pairing interaction in the ferropnictide materials have attempted to calculate the momentum dependence of the order parameter associated with the leading superconducting instability. Using a 5 Fe-orbital model, Kuroki *et al.*³⁹ performed an RPA calculation of the interaction to construct a linearized gap equation, and determined that the leading pairing instability had s -wave (A_{1g}) symmetry, with nodes on the electron-like Fermi surface (“ β sheets”). Wang *et al.*⁴⁰ studied the same pairing problem within a 5-orbital framework using the functional renormalization group approach, also finding that the leading pairing instability is in the A_{1g} -wave channel, and that the next leading channel had B_{1g} ($d_{x^2-y^2}$) symmetry. For their interaction parameters, they found no nodes on the Fermi surface, but nevertheless a significant variation of the magnitude of the gap. Graser *et al.* also performed a 5-orbital RPA framework⁴¹, using the DFT bandstructure of Cao *et al.*⁴⁸ as a starting point. These results indicated that the leading pairing channels were indeed of s (A_{1g}) and $d_{x^2-y^2}$ symmetry, and that one or the other could be the leading eigenvalue, depending on details of interaction parameters. More recently, several authors have investigated the factors including intrasheet Coulomb interaction, nesting of electron pockets, and orbital character of pairing which can influence order parameter anisotropy within these models^{42,43,44}. Other approaches have also obtained A_{1g} gaps which change sign between the hole and electron Fermi surface sheets

but remain approximately isotropic on each sheet^{45,46}.

In this paper we calculate the expected thermal conductivity in superconducting states potentially appropriate to the ferropnictide superconductors. We adopt for convenience a phenomenological 2-band model, allowing order parameters on two Fermi surface sheets representing the hole- and electron-doped sheets found in density functional theory calculations for these materials. We consider the region outside of the doping range where superconductivity may coexist with antiferromagnetism. Our model for disorder consists of terms allowing for scattering within (intraband) and between (interband) Fermi surface sheets, of arbitrary strength. This allows us to control the width and position of the impurity band in both nodal pairing states and those with a fully developed spectral gap, which we examine with a view towards determining the size and universality of the linear- T term in κ at the lowest temperatures. After examining the zero-field situation, we discuss the effect of an applied field. To this end we adopt the method of Brandt-Pesch-Tewordt to obtain predictions for the widest possible field range. We illustrate the various possibilities of superconducting state and disorder types which allow the results observed thus far in experiments.

II. MODEL

We begin by assuming a metallic system with two bands 1 and 2, characterized by densities of states N_1 and N_2 at the Fermi level, and a pair interaction which is a sum of separable terms,

$$V(\mathbf{k}, \mathbf{k}') = V_1 \Phi_1(\mathbf{k}) \Phi_1(\mathbf{k}') + V_2 \Phi_2(\mathbf{k}) \Phi_2(\mathbf{k}') + V_{12} [\Phi_1(\mathbf{k}) \Phi_2(\mathbf{k}') + \Phi_2(\mathbf{k}) \Phi_1(\mathbf{k}')], \quad (1)$$

where Φ_i is function of A_{1g} symmetry depending on momentum restricted to band $i = 1, 2$.

For disorder we will assume an orbital-independent matrix element which scatters quasiparticles either within a given band with amplitude U_{ii} , $i = 1, 2$, or between bands with amplitude U_{12} . As discussed in the appendix, we sum all single-site scattering processes of arbitrary strength to obtain a disorder-averaged Nambu self energy $\underline{\Sigma} = n_{imp} \underline{T}$, where n_{imp} is the concentration of impurities. For simplicity, we assume $U_{11} = U_{22} \equiv U_d$, with equal densities of states $N_i = N_0$ throughout the paper. In our preliminary considerations we restrict ourselves to purely intraband scattering, $U_{12} = 0$. The disorder is characterized by two intraband scattering parameters on each sheet: $\Gamma_i \equiv n_{imp}/(\pi N_i)$ and $c_i = 1/(\pi N_i U_{ii})$; For our simple initial case with 2 symmetric bands we set $\Gamma_i = \Gamma$ and $c_i = c$, $i = 1, 2$. The initial neglect of interband scattering may be understood in zeroth order by noting that a screened Coulomb potential with screening length of order a unit cell size will generically have larger small- \mathbf{q} compared to large- \mathbf{q} scattering. The real situation is somewhat more complex since the same orbitals contribute to both electron

and hole Fermi surface sheets⁴¹, and therefore a substitutional impurity, such as Co, may be expected to produce a significant interband scattering component as well. Hence we relax this requirement and below also analyze the regime $U_{12} \simeq U_d$, and, in particular, the case $U_{12} = U_d$, as discussed in Ref.35. Weak interband scattering $U_{12} \ll U_{11}, U_{22}$ does not qualitatively change the results obtained in the limit $U_{12} = 0$.

The full matrix Green's function in the presence of scattering in the superconducting state is given by a diagonal matrix in band space, as discussed in the appendix,

$$\underline{G}(\mathbf{k}, \omega) = \frac{\tilde{\omega}\tau_0 + \tilde{\epsilon}_{\mathbf{k}}\tau_3 + \tilde{\Delta}_{\mathbf{k}}\tau_1}{\tilde{\omega}^2 - \tilde{\epsilon}_{\mathbf{k}}^2 - \tilde{\Delta}_{\mathbf{k}}^2}, \quad (2)$$

where $\mathbf{k} = \mathbf{k}_i \in S_i$ is restricted to Fermi surface sheet S_i with $i = 1, 2$, and the renormalized quantities $\tilde{\omega} \equiv \omega - \Sigma_0$, $\tilde{\epsilon}_{\mathbf{k}} \equiv \epsilon_{\mathbf{k}} + \Sigma_3$, $\tilde{\Delta}_{\mathbf{k}} \equiv \Delta_{\mathbf{k}} + \Sigma_1$ also depend on the band indices through \mathbf{k} . The Σ_α are the components of the self-energy proportional to the Pauli matrices τ_α in particle-hole (Nambu) space.

Below we focus on two quantities. It is useful to start with the analysis of the total density of quasiparticle states (DOS)

$$\begin{aligned} N(\omega) &= -\frac{1}{2\pi} \text{Tr} \text{Im} \sum_{\mathbf{k}} \underline{G}(\mathbf{k}, \omega) \\ &= -\frac{1}{2\pi} \text{Tr} \sum_i \sum_{\mathbf{k}_i} \underline{G}(\mathbf{k}_i, \omega), \end{aligned} \quad (3)$$

where the second equality indicates the explicit integration over distinct Fermi surface sheets with momenta \mathbf{k}_i . We will be comparing results for the DOS with thermal conductivity κ calculated using the standard approach⁴⁷,

$$\begin{aligned} \kappa &= \sum_i \frac{N_i v_{Fi}^2}{8} \int_0^\infty d\omega \frac{\omega^2}{T^2} \text{sech}^2\left(\frac{\omega}{2T}\right) \\ &\times \left\langle \frac{1}{\text{Re}\sqrt{\tilde{\Delta}_i^2 - \tilde{\omega}_i^2}} \left[1 + \frac{|\tilde{\omega}_i|^2 - |\tilde{\Delta}_i|^2}{|\tilde{\Delta}_i^2 - \tilde{\omega}_i^2|} \right] \right\rangle_\phi. \end{aligned} \quad (4)$$

Here $\langle \dots \rangle_\phi$ is average over the Fermi surface sheet, \sum_i denotes the sum over the bands, and v_{Fi} is the Fermi velocity on sheet i . We assume cylindrical Fermi surfaces, so that \mathbf{v}_{Fi} is isotropic.

III. ISOTROPIC A_{1g} STATES

We first discuss the thermal conductivity in isotropic s -wave or A_{1g} states. If the sign of the order parameter Δ is the same on both sheets, and no magnetic disorder is present, the low- T thermal conductivity will be similar to classic calculations for conventional superconductors, and yield an exponential low- T dependence for the electronic part. In the case of a sign-changing s (" s_\pm ") state proposed by Mazin et al.⁴⁵, the situation is more interesting. Here one assumes an isotropic Δ_i on each sheet

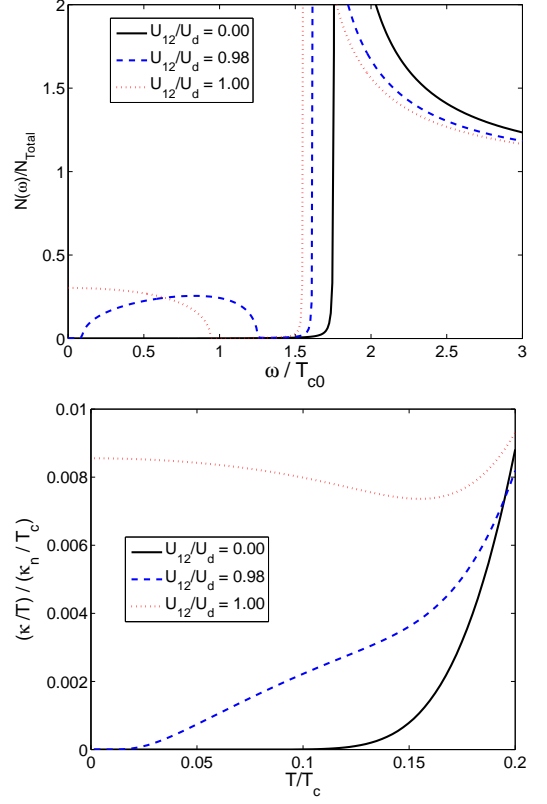


FIG. 1: Density of states (a) and thermal conductivity (b) for an isotropic s_\pm state with $\Delta_1 = -\Delta_2$, shown for $U_d = U_{11} = U_{22}$ (intraband Scattering) and scattering rate parameters $c = 0.07$ and $\Gamma = 0.3T_{c0}$ in cases (i) weak intraband scattering only, $U_{12}/U_d = 0$ (solid line); (ii) pairbreaking scattering with midgap impurity band, $U_{12}/U_d = 0.98$ (dashed line); (iii) pairbreaking scattering with impurity band overlapping Fermi level, $U_{12}/U_d = 1.0$ (dotted line).

i , but assumes that $\text{sgn}\Delta_1 = -\text{sgn}\Delta_2$. In terms of Eq. 1, we choose the functions $\Phi_i(\mathbf{k}) = 1$ for $\mathbf{k} \in S_i$ and zero otherwise, and fix the sign of V_{12} to be opposite to that of V_1, V_2 so as to induce a sign-changing order parameter between the two sheets. In the clean case, we continue to expect an exponential or full gapped dependence to the thermal conductivity. On the other hand, in such systems ordinary disorder is pairbreaking if it includes a strong interband component^{33,34,35,36}. For some situations a low-energy impurity band may indeed give rise to a linear term in the thermal conductivity.

For simplicity, we assume that $\Delta_2 = -\Delta_1 \equiv \Delta$, and equal densities of states on the two bands. In Fig. 1, we now illustrate the correspondence between the formation of the impurity band in the fully gapped state, and the creation of the linear term. In the absence of interband scattering, there is no pairbreaking in the sense of Anderson's theorem, and the spectral gap in the DOS is identical to the unrenormalized order parameter Δ , corresponding to an activated thermal conductivity

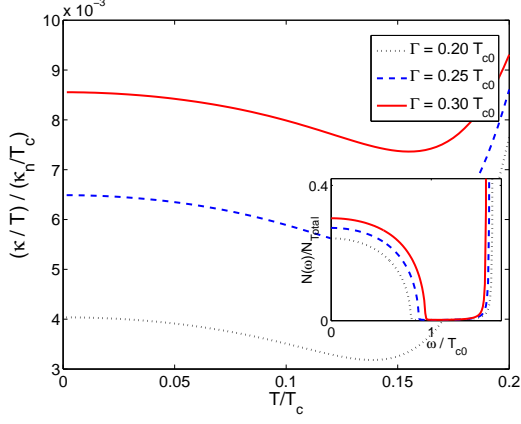


FIG. 2: Density of states (insert) and thermal conductivity for an isotropic s_{\pm} state with scattering parameters as Fig. 1 but $U_{12}/U_d=1.0$ and $\Gamma = 0.2, 0.25$, and $0.3T_{c0}$.

$\sim \exp(-\Delta/T)$. As interband scattering is increased, states are pulled down from the continuum into the gap, creating eventually a band of midgap states in the DOS, as shown. If there is still a narrow energy range which is gapped near the Fermi level, this smaller gap determines the slower but still exponential decrease of κ at the lowest temperatures. As soon as the impurity band of midgap states overlaps the Fermi level, a linear term in κ appears^{34,55}. Note that a significant interband component of scattering essentially equal to the intraband component is absolutely necessary for this to occur, which requires special conditions as described above.

We note further that if one varies the concentration of impurities in the situation with $U_{12} = U_d$, the change in the residual density of states $N(0)$ is reflected directly in the slope of the thermal conductivity, as shown in Fig. 2. This is not surprising but is in dramatic contrast to the universal (disorder-independent) behavior observed in d -wave superconductors. This raises the question of the degree of universality of transport coefficients in pairing states which have s -wave (A_{1g}) character but also display nodes.

IV. ANISOTROPIC A_{1g} STATES

We now examine states within the same A_{1g} symmetry class, but where gap minima are either very deep, with no sign change, or with actual sign change (nodes). To make contact with microscopic theory (see e.g. Ref. 41), we assume that one of the sheets (in microscopic theory, the so-called “ α ” sheet around the Γ point) has an isotropic order parameter while the other (the “ β ” sheet around the M point) has a highly anisotropic one. In this case, the order parameters in the two bands are given by

$$\Delta_1 = -\Delta \quad (5)$$

$$\Delta_2 = \Delta_{iso} + \Delta_{ani} \cos 2\phi, \quad (6)$$

where ϕ is the angle around the electron Fermi surface sheet 2. It is useful to define the gap ratio in the electron-like band, $r \equiv \Delta_{ani}/\Delta_{iso}$, so that $r > 1$ ($\Delta_{ani} > \Delta_{iso}$) gives a state with nodes in that band, while $r < 1$ ($\Delta_{ani} < \Delta_{iso}$) has none.

To obtain this order parameter from Eq. (1), we choose

$$\Phi_1(\mathbf{k}) = \begin{cases} 1 & \mathbf{k} \in S_1 \\ 0 & \text{otherwise} \end{cases} \quad (7)$$

$$\Phi_2(\mathbf{k}) = \begin{cases} 1 + r_V \cos(2\phi) & \mathbf{k} \in S_2 \\ 0 & \text{otherwise} \end{cases}, \quad (8)$$

where as before, S_1 and S_2 represent the hole and electron Fermi surfaces, respectively. In the clean limit, the gap equation is

$$\Delta_i(\phi) = 2\pi T \sum_{\omega_n} \Phi_i(\phi) \times \sum_j \int_{\phi' \in S_j} N_j V_{ij} \Phi_j(\phi') \frac{\Delta_j(\phi')}{\sqrt{\omega_n^2 + \Delta_j^2(\phi')}} \quad (9)$$

where ω_n are fermionic Matsubara frequencies. Below we adjust the value of r_V to study a nodal system with $r = 1.3$ and an anisotropic state with no nodes with $r = 0.9$.

In the presence of disorder, we evaluate the impurity average self energies $\Sigma_{i,\alpha}$ for both the bands, where again i is the band index and α is the Nambu index. This calculation is detailed in the Appendix, with the results presented in Eqs.(A8)-(A11). Since the structure of the order parameter in the clean limit already supports low-energy excitations, we first ignore the interband scattering in the first analysis, and focus on the effects of intraband scattering alone. We define the conventional renormalized quantities

$$\tilde{\omega}_i = \omega - \Sigma_{i,0} \quad i = 1, 2 \quad (10)$$

$$\tilde{\Delta}_i = \Delta_i + \Sigma_{i,1}, \quad (11)$$

where in each case the first subscript is a band index, while the second one is a Nambu index. Since the self energy is \mathbf{k} -independent in this approximation, we can associate the self-energy with the renormalization of the isotropic component, $\tilde{\Delta}_{iso} = \Delta_{iso} + \Sigma_{2,1}$, but this is simply a matter of convenience. The total thermal conductivity comes from sum over both bands, but at very low temperatures the contribution from the first band is very small due to the fully developed gap assumed.

A. A_{1g} states with nodes

We first discuss the situation where $\Delta_2(\mathbf{k})$ has nodes but a non-zero average over the Fermi surface, and for concreteness take $r = 1.3$. The behavior of the low- T thermal conductivity with increasing disorder for a case with individual scatterers near the strong potential limit is now shown in Fig. 3.

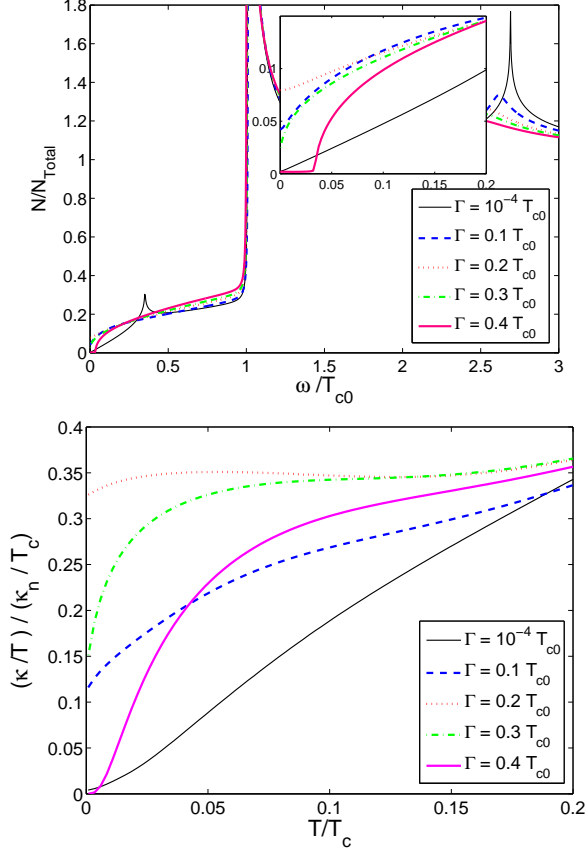


FIG. 3: Density of states $N(\omega)/N_{Total}$ (top) and normalized thermal conductivity $(\kappa(T)/T)/(\kappa_n/T_c)$ vs. T/T_c for two band anisotropic model with isotropic order parameter on sheet 1 and anisotropic order parameter $\Delta_1 = -1.1 T_{c0}$ on sheet 1 and $\Delta_{iso} = 1.3 T_{c0}$, $r = 1.3$ on sheet 2 (Eq. (6)). Results shown for various values of intraband scattering rate Γ/T_{c0} and $c = 0.07$, and no intraband scattering, $U_{12} = 0$.

The evolution of $\kappa(T)$ is very different from that for a pure d -wave superconductor. This is clearly seen from the evolution of the $T = 0$ limit of the thermal conductivity. In the pure case the linear term is nearly invisible. As intraband disorder is increased, the linear term significantly increases in magnitude, goes through a maximum and eventually disappears, leading to an exponential temperature dependence. To some extent this behavior can be understood by examining the corresponding density of states, as shown in the upper panel; as disorder increases, the nodal quasiparticle states are broadened and a residual density of states appears, but as disorder is increased further the nodes are lifted and a fully developed spectral gap appears, as discussed in Ref. 38.

To clarify why there is no “universal independence” of weak disorder expected, e.g. for d wave superconductors^{49,50,51}, we plot in Fig. 4 the value of the asymptotic low- T limiting value of κ/T as a function of disorder; there is, for this case, no range of disorder where the behavior can in any sense be called univer-

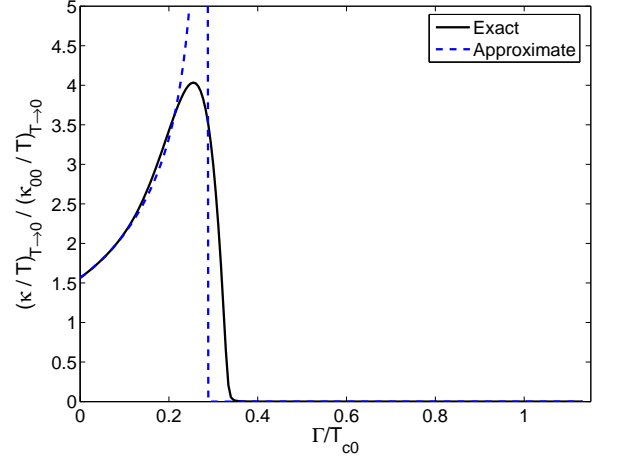


FIG. 4: Magnitude of linear- T term in thermal conductivity in limit $T \rightarrow 0$ for case with nodes $r = 1.3$, plotted as a function of intraband scattering rate Γ/T_{c0} for $c = 0.07$. Solid line: exact numerical result. Dashed line: analytical estimate from text, Eq. (14). Here κ_0 is the thermal conductivity for a d -wave superconductor, with order parameter $\Delta(\phi) = \Delta_{ani} \cos 2\phi$. Δ_{ani} is same as anisotropic component in clean system for the model specified by Eq. (6).

sal. This result is somewhat similar to that in Ref. 52 where the effect of an orthorhombic distortion on the in plane thermal conductivity of $YBCO$ was studied. Note that in their case the s -wave component of the $d + s$ order parameter breaks A_{1g} symmetry in the ab -plane. In our case A_{1g} is preserved because there are two β sheets whose nodal structures are rotated with respect to each other by 90 degrees⁴¹.

To analyze the origin of the breakdown of universality in the anisotropic A_{1g} state, we evaluate the $T \rightarrow 0$ limit by replacing the derivative of the Fermi function by a delta function and integrating over the energy ω . The isotropic band 1 does not contribute to the thermal conductivity at very low temperature because it is fully gapped. The main contribution comes therefore from the nodal states from band 2. In contrast to a d -wave superconductor, here the anomalous self-energy $\Sigma_{2,1}$ is finite, therefore the compensation between the density of states and the scattering rate does not occur, and the universal behavior breaks down. As a result, the position of the nodes on the Fermi surface shifts, and the slope of the gap changes.

If we linearize the gap near the node, $\tilde{\Delta}(\phi) \approx k_F v_{\Delta}(\phi_0 - \phi)$, where ϕ_0 is the location of node, determined from $\cos 2\phi_0 = -[\Delta_{iso} + \Sigma_{2,1}(\omega = 0)]/\Delta_{ani}$, the renormalized gap slope is

$$v_{\Delta} = 2k_F^{-1} \Delta_{ani} \sin(2\phi_0) \quad (12)$$

$$= 2k_F^{-1} \sqrt{\Delta_{ani}^2 - (\Delta_{iso} + \Sigma_{2,1}(\omega = 0))^2}. \quad (13)$$

Summing over the nodes, we find

$$\frac{\kappa}{T} \approx \frac{N v_F^2 \pi}{3} \frac{2}{k_F v_\Delta}, \quad (14)$$

which has precisely the same form as the well-known d -wave result (to leading order in v_Δ/v_F), *except* that the gap velocity v_Δ , which is unrenormalized by disorder in the d -wave case, is strongly disorder dependent here due to the nonzero off-diagonal impurity self-energy $\Sigma_{2,1}$ in Eq. 13. The increase in the residual thermal conductivity is therefore due to the flattening of the gap in the near nodal region before the system becomes fully gapped at higher impurity scattering rates. The absence of the residual linear term in this picture is only consistent with a sufficiently high disorder, when the spectral gap is finite.

B. Anisotropic states with deep gap minima

An alternative scenario for the absence of a linear term in $\kappa(T)$ in K-, Ni- and Co-doped 122 ferropnictide materials^{28,29,37}, is a highly anisotropic state on at least one of the Fermi surface sheets with deep minima but no true nodes. Here we choose $\Delta_{ani} < \Delta_{iso}$ ($r = 0.9$) to simulate a situation where the clean state is slightly gapped, and varies between a minimum value of $\Delta_{iso} - \Delta_{ani}$ and $\Delta_{iso} + \Delta_{ani}$. Again we begin by including only intraband impurity scattering, for which the results are shown in Fig. 5. In this case, disorder merely increases the spectral gap due to averaging, as discussed in Ref. 38, leading to an increasingly rapid exponential decay.

If interband scattering is included, low-energy states appear, similarly to the s_\pm case considered above, but again we find that the values of interband scattering strength U_{12} near the intraband value U_d are necessary to create such states sufficiently near the Fermi level to create a linear term in κ . For simplicity, therefore, we take both inter and intra band scattering potentials to be equal, i.e. the scattering is isotropic in momentum space. For intermediate to strong potentials, states are then created near the Fermi level. It is important to remember that such scattering rapidly suppresses T_c , as illustrated in Fig. 6. The next figure exhibits the thermal conductivity for this system. Because the pure system has a small spectral gap, even the smallest disorder in this limit gives rise to an impurity band close to the Fermi level, creating unpaired quasiparticles. For significant impurity concentrations, a strong linear term appears which also of course violates universality, as shown explicitly in Fig. 7. The variation of this linear term with disorder for isotropic scattering is shown in Fig. 8 and compared to an approximation where we made a series expansion around $\pi/2$ for Δ_ϕ . We find

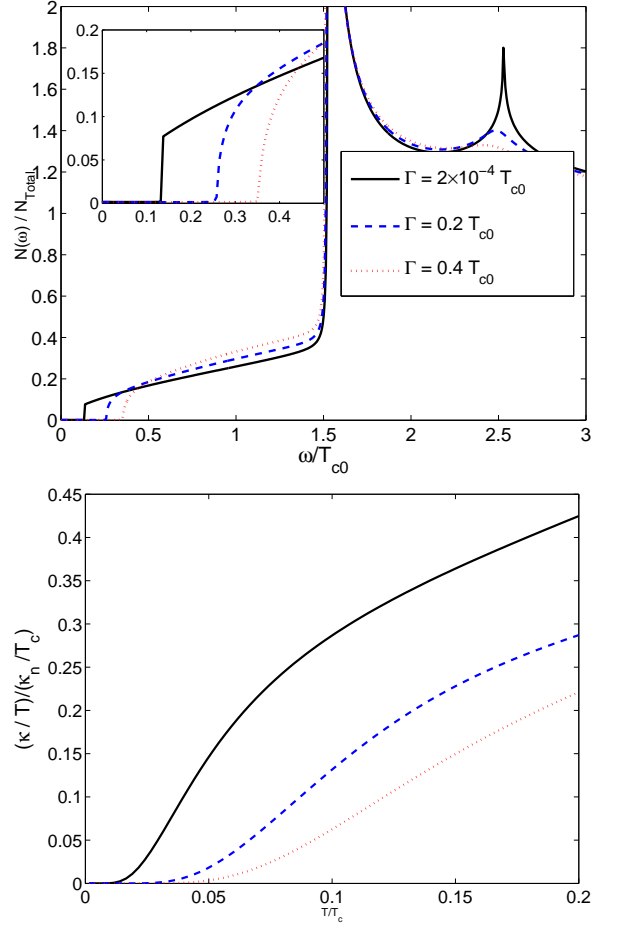


FIG. 5: (Top) Normalized density of states $N(\omega)/N_0$ vs. ω/T_{c0} for two band anisotropic model with isotropic gap on sheet 1 and $r = 0.9$ (deep gap minima) on sheet 2 (Eq. (6)). Results are shown for various values of intraband scattering rate Γ/T_{c0} and $c = 0.07$. Bottom: normalized thermal conductivity $(\kappa(T)/T)/(\kappa_n/T_c)$ vs. T/T_c .

$$\begin{aligned} \frac{\kappa}{T} \approx & \frac{N_2 v_{F2}^2 \pi}{6} \frac{\Gamma_2^2}{\Gamma_2^2 + (\Delta_{iso} + \Sigma_{2,1} - \Delta_{ani})^2} \\ & \times \frac{1}{\sqrt{\Delta_{ani} (\Delta_{iso} + \Sigma_{2,1} - \Delta_{ani})}} \\ & + \frac{N_1 v_{F1}^2 \pi^2}{6} \frac{\Gamma_1^2}{(\Gamma_1^2 + (\Delta + \Sigma_{1,1})^2)^{3/2}}, \end{aligned} \quad (15)$$

where Γ_i are the normal state scattering rates defined above, and all the self-energies are evaluated at $\omega = 0$. Note that there now appears a contribution from the isotropic band 1 because Eq. 15 assumes the isotropic scattering condition $U_{11} = U_{12}$, which leads to strong pairbreaking and quasiparticle states near the Fermi level. Consequently, the absence of the residual linear term in κ is also consistent with the deep minima provided the interband scattering is not too strong. We now

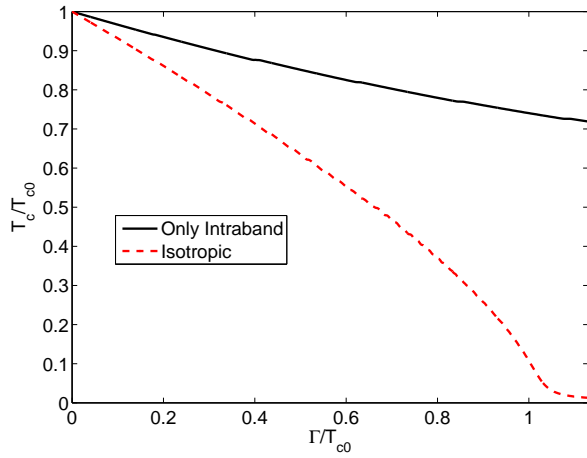


FIG. 6: Comparison of the effects of intraband and isotropic scattering on T_c . Solid curve is pure intraband scattering T_c/T_{c0} vs. Γ/T_{c0} for $U_{12} = 0$; dashed curve is same, but for $U_{12} = U_{11} = U_{22}$.

proceed to investigate the field dependence in the two cases.

V. FIELD DEPENDENCE

Thermal conductivity depends on the applied magnetic field since the density of unpaired electrons depends on the field magnitude. These electrons carry entropy and hence enhance the heat current. They also scatter phonons and therefore reduce the lattice contribution to the thermal transport, so that the two effects compete. On general grounds, $\kappa(T, H)$ that increases at low temperatures with applied field can be assumed to contain a substantial electronic component²⁵. In some systems, such as heavy fermion metals, the electron contribution to the thermal conductivity is dominant, allowing a direct probe of the heat transport in the superconducting state throughout the T - H plane⁷³. In other materials, where the phonon contribution is substantial, the quantity that lends itself most easily to analysis is the *residual* linear term in the thermal conductivity, $\lim_{T \rightarrow 0} \kappa/T$, which is purely electronic since the phonon contribution vanishes in that limit^{74,75,76}.

Therefore, for the purposes of comparison with experiment, we focus on the field dependence of the electronic thermal conductivity at low temperature. In nodal superconductors, where the transport is dominated by bulk quasiparticles with momenta nearly along the nodal directions, two methods have been employed to describe this dependence. The semiclassical approach is based on the observation that the energy to break a Cooper pair is lowered outside of the vortex core since the unpaired electrons do not participate in the supercurrent flowing around the vortex. Hence effect of the field can be described by the Doppler shift of the quasiparticle energy,

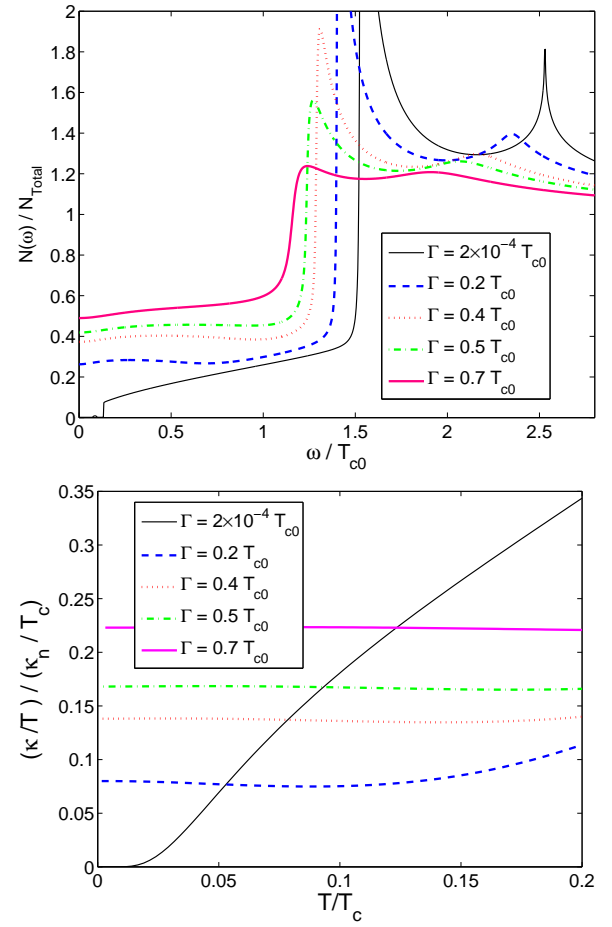


FIG. 7: Density of states $N(w)/N_0$ (top) and normalized thermal conductivity $\kappa(T)T_c/(\kappa_n T)$ vs. T/T_c for two band anisotropic model with isotropic order parameter on sheet 1 and $r = 0.9$ (deep gap minima) on sheet 2 (Eq. (6)). Results are shown for equal intraband and interband scattering $U_{12} = U_d$.

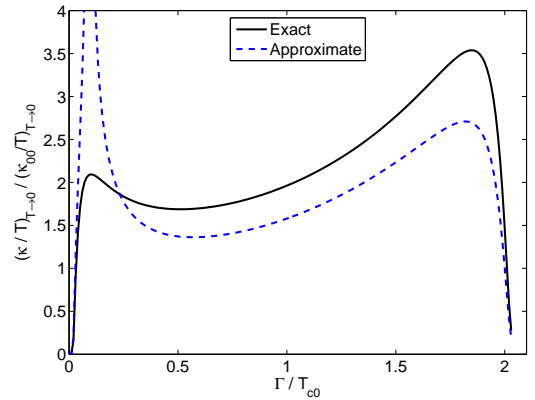


FIG. 8: κ/T in $T \rightarrow 0$ limit, for the state with deep gap minima. κ_0 is thermal conductivity for pure d-wave state. Band 1 has isotropic order parameter $\Delta = -1.7 T_{c0}$ and band 2 has $r = 0.9$ and $\Delta_{iso} = 1.5 T_{c0}$ on it.

$\mathbf{v}_s(\mathbf{r}) \cdot \mathbf{k}_F$, where $\mathbf{v}_s(\mathbf{r})$ is the supervelocity field determined by the vortex structure^{77,78,79}. This energy shift is local, and therefore the method is very well suited for describing the thermodynamic quantities, but requires additional assumptions to account for correlation functions and transport properties^{80,81,82,83}. It is applicable at low energies and therefore restricted to low temperatures and fields.

An alternative approach assumes the existence of the vortex lattice and describes the behavior starting from the moderate to high field regime. The approximation consists of replacing the diagonal, in Nambu space, components of the Green's function with their averages over the unit cell of the vortex lattice, while keeping the exact spatial dependence of the off-diagonal, Gor'kov components. It was developed for conventional superconductors by Brandt, Pesch, and Tewordt^{84,85}, who showed that the replacement is valid since the Fourier components of the Green's function (in reciprocal lattice vectors of the vortex lattice, \mathbf{K}), vary as $G_{\mathbf{K}} \propto \exp(-\Lambda^2 K^2)$, where $\Lambda^2 = \hbar c / eB$ is the magnetic length, which is of order of the intervortex distance. The method gives excellent agreement with experimental results on both thermodynamic and transport properties superconductors near the upper critical field^{86,87}, and remains semi-quantitatively correct in s -wave superconductors down to fields of less than half of H_{c2} ⁸⁸. It fails at the lowest fields, when the unpaired electrons are localized in the vortex cores, and consequently cannot be described by the propagators averaged over the (much greater) unit cell size. In this low field limit, the method gives an artificially enhanced behavior of the thermal conductivity as it treats the localized states as extended, and generically produces power law increase in $\kappa(H, T)$, while both the expected and the experimentally observed initial increase in $\kappa(H, T)$ is exponentially small.

In contrast, the extension of the BPT method to the nodal superconductors^{89,90,91,92,93} remains valid down to lowest fields since even in that regime the transport is dominated by the extended states. It gives results qualitatively and quantitatively consistent with the Doppler shift method^{94,95}, and hence describes the properties over nearly the entire range of the temperatures and fields. We employ this method here.

We extend the approach of Ref.93 to the two-band model. The matrix Green's functions of the electron and hole bands are coupled by the self-consistency equation on the order parameter and the T -matrix as shown in Eq.(9) and Eqs.(A8)-(A11). We model the vortex lattice as^{91,92}

$$\Delta_i(\mathbf{R}, \phi) = \sum_{k_y} C_{k_y} \Phi_i(\phi) e^{ik_y y} F_0 \left(\frac{x - \Lambda^2 k_y}{\Lambda} \right), \quad (16)$$

where F_0 is the ground state oscillator wave function, the coefficients C_{k_y} determine the structure of the vortex state and the amplitude of the order parameter, and i is the band index. Since the bands are treated as separate, the thermal conductivity is the sum of the contributions

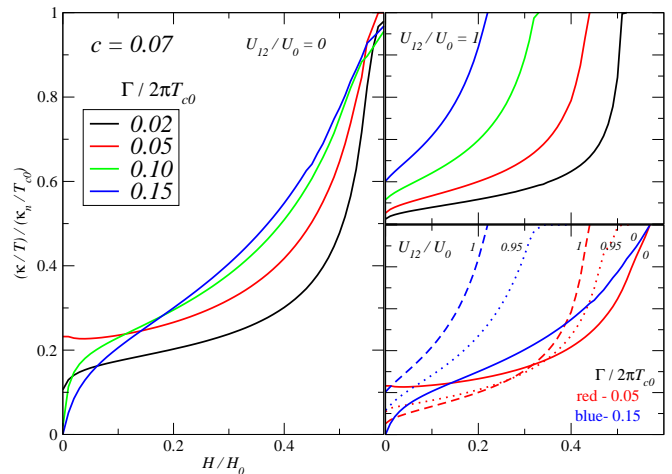


FIG. 9: (Color online) The field dependence of the thermal conductivity at $T = 0.02T_{c0}$ for the order parameter with nodes, $r = 1.3$. Left panel: Intraband scattering only for different scattering rates near the unitarity limit. Right panel top: the same in the presence of strong interband scattering. Right panel bottom: evolution of the field dependence with increased interband scattering.

due to the hole and the electron sheets of the Fermi surface.

Our approach is most reliable for the states with nodes in the gap function, when the results can be trusted over essentially the entire field range. Note that even though the hole band is always fully gapped in our analysis, at low fields the dominant contribution is from the electron band with gap nodes. The main feature in the field dependence, as shown in Fig. 9 is the pronounced inflection point at low fields where a crossover from a rapid rise to a slower increase occurs. This result bears striking resemblance to the recent measurements on LaFePO superconductor³¹, which were interpreted precisely in the framework of the two-band picture, with one band possessing nodes in the gap.

This rapid increase is related to a significant variation in the density of states with energy in zero field, shown in Fig. 3. The corresponding thermal conductivity for the parameter values chosen here also exhibits a shoulder as a function of temperature at low T . This shoulder is not found experimentally in Ref. 31, but we have to keep in mind that, if the sample contains non-superconducting regions, the residual linear term may not be related to the superconducting phase, while the field enhancement at low T is still determined by the increase in the number of unpaired electrons.

Note also that when the residual linear- T term is near its maximal value in Fig. 4, which for parameters here occurs near $\Gamma/2\pi T_{c0} \simeq 0.05$, the field and temperature dependence of $\kappa(T, H)$ is very weak, more reminiscent of that of a fully gapped superconductor. The nodes however are not lifted up to a higher impurity concentration,

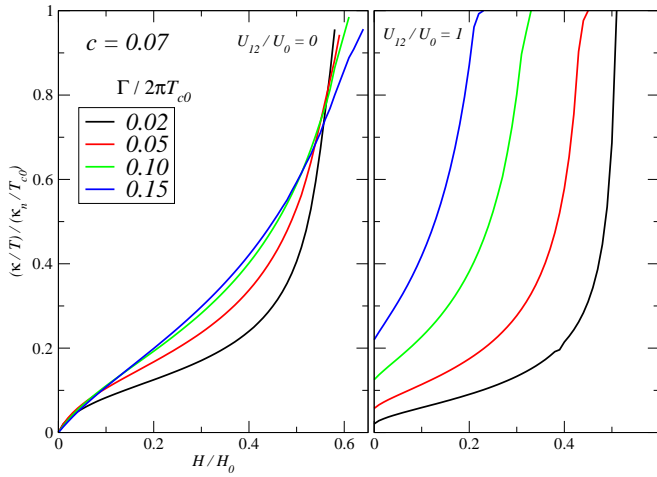


FIG. 10: (Color online) The field dependence of the thermal conductivity at $T = 0.02T_{c0}$ for the order parameter with deep minima, $r = 0.9$. Left panel: Intraband scattering only. Right panel: the strong interband scattering.

$\Gamma/2\pi T_{c0} \simeq 0.08$. The reason for this is clear from comparisons with Ref.38: as the slope of the gap near the node becomes small, the shape of the gap function deviates from a simple cosine, and becomes very steep beyond the near-nodal region, so that moderate field essentially does not excite additional quasiparticles.

In general, we do need to keep in mind that, as the nodes are lifted, the applicability of the BPT approximation at low fields becomes questionable, but the minimal gap in the regime we show here, $\Gamma/2\pi T_{c0} \leq 0.15$, is small, and therefore the method remains reliable to very low fields. Quite generally, the energy scales associated with the effect of magnetic field on the extended quasiparticles are of order $E_0 \sim \Delta\sqrt{H/H_{c2}}$, so that for the $\Delta_{min}/\Delta \sim 0.1$ we expect the extended states to dominate the response for $H/H_{c2} \geq 0.01$. Consequently, we trust the approximation even in the regime when the nodes are lifted.

This argument allows us to extend the treatment to the state with the deep minima, rather than the true nodes. We consider once again $r = 0.9$ and show the results in Fig. 10. As can be expected from a probe that is sensitive to the amplitude, rather than the phase, of the gap function, the overall features are quite similar to those for a true nodal gap. The low-field inflection and the rapid rise are not as clearly pronounced, consistent with the absence of true nodal quasiparticles until the field is sufficiently high. As pointed out above, for the nodeless state the inclusion of strong interband scattering leads to a rapid enhancement in the residual density of states, and the concomitant increase in the residual linear term in the thermal conductivity.

Finally, in Fig. 11 we show the results for the isotropic s_{\pm} state. While in this case we do not trust our approximation at low fields, it is clear that the increase

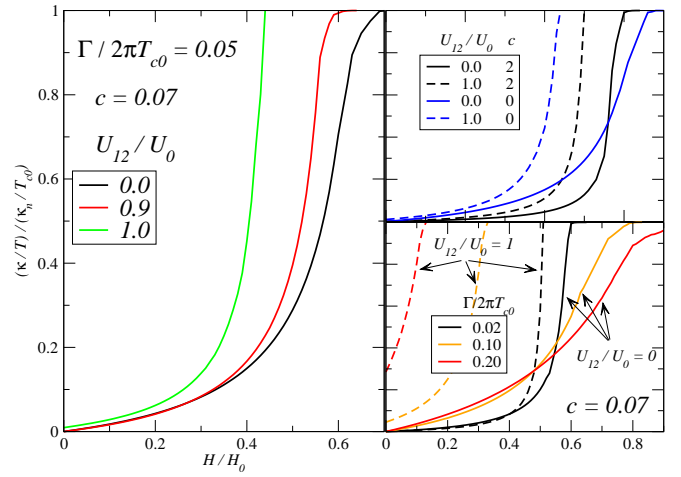


FIG. 11: (Color online) The field dependence of the thermal conductivity for the s_{\pm} state. Left panel: clean case near the unitarity limit. Right panel top: influence of the phase shift of scattering on the low-field behavior. Right panel bottom: evolution of the field dependence with interband scattering.

in the thermal conductivity with the magnetic field is much slower than for the two cases considered above. To require an even moderately rapid growth of $\kappa(H)$ at low fields requires a substantial residual linear term as well as unphysically high interband scattering, see bottom right panel of Fig. 11. This result strongly suggests that the isotropic s_{\pm} state is incompatible with the results of Ref.²⁸ on the 122 series of materials, just as the results of Ref.³¹ exclude this order parameter structure in the LaFePO system.

VI. CONCLUSIONS

We have argued that thermal conductivity is the ideal probe to resolve current apparent discrepancies between various thermodynamic and spectroscopic measurements on the Fe-based superconductors. In particular, since several of these experiments indicate the existence of low-lying quasiparticle states in certain materials, it is important to settle whether or not these excitations extend all the way down to the Fermi energy, or whether there is a true spectral gap in the system. Thermal conductivity, a bulk probe, is currently measurable to lower temperatures than other probes, so it may be able to settle this dispute and also distinguish between two popular scenarios. The two most likely order parameters for these systems appear at present to be the isotropic s_{\pm} state proposed by Mazin et al.⁴⁵, and highly anisotropic A_{1g} states, with nodes or deep gap minima, found in spin fluctuation calculations. The former state can be consistent with the reports of low-lying excitations only if pairbreaking disorder induces an impurity band, while the latter are difficult to reconcile with ARPES experi-

ments indicating a large spectral gap in some materials.

We have therefore calculated the thermal conductivity of a superconductor with A_{1g} symmetry order parameter in a model 2-band system, and considered the effects of intra- and interband disorder. In zero field, we have shown that the linear T term which dominates $\kappa(T)$ at low temperatures has a coefficient which is nonuniversal (unlike the well-known d -wave case) and depends non-monotonically on disorder. Details depend on the precise order parameter structure of the model pure system, and on location of the impurity band in the DOS. The linear- T term in zero field found in the LaFePO material³¹, is consistent in principle with the linear- T penetration depth observed in the same system⁸ and suggestive of nodes in the superconducting order parameter. This term is rather large as a fraction of the normal state thermal conductivity. While within the present theoretical approach realistic evaluation of the normal state κ is difficult, as we have neglected both phonons, which would enhance this contribution, and inelastic electronic scattering, which would suppress it, it seems likely that it would be difficult to account for its size within the current framework, and it is possible, as Ref. 31 mentions, that it is of extrinsic origin. In the 122 systems, the extremely small or zero linear- T term^{28,29} suggests a true spectral gap, consistent either with an isotropic s_{\pm} state or a gap with deep minima.

An examination of the field dependence of the low temperature thermal conductivity within the BPT approach has enabled us to draw further conclusions. The size of the initial field dependence seen in experiment rules out a clean s_{\pm} state as a possible candidate for the 122 materials. However, as pointed out in the context of other experiments, pairbreaking scattering can induce a low-lying impurity band in such a state, and produce responses similar to highly anisotropic states. We have analyzed this situation and found that the amount of pairbreaking (intraband) scattering required to reproduce the observed field dependence is large. In most situations this is unphysical, both in the sense that the ratio of interband to intraband scattering must be tuned to a special value (which seems unreasonable in the context of screened Coulomb scattering), and because a very large concomitant T_c suppression would be produced. As mentioned above, an argument for a sizeable interband scattering component may be made for Co-doped systems, but the general argument against fine-tuning to a special value still holds, and the experimental agreement between the behavior of the thermal conductivity on systems with different dopants indicates the generic features of the material. The evolution of the thermal conductivity with Co doping³⁷, however, may be at least in part due to the strong interband scattering component. We therefore conclude that the most likely candidate for the order parameter in the 122 materials is a highly anisotropic A_{1g} state with deep gap minima, probably on the electron (“ β ”) sheets. How this conclusion can be reconciled with ARPES experiments is not clear at this writing. We

emphasize that controlled disorder not associated with doping, such as electronic irradiation, would provide the best test of the predictions of our theory.

Acknowledgments

The authors are grateful for useful communications with L. Taillefer and Y. Matsuda. PJH is grateful for the hospitality of the Kavli Institute for Theoretical Physics during the preparation of this manuscript. Research was partially supported by DOE DE-FG02-05ER46236 (PJH) and DOE DE-FG02-08ER46492 (IV).

APPENDIX A: BASIC FORMALISM

For low impurity concentrations, one can ignore the processes which involve scattering from multiple impurity sites. Within this single site approximation, we sum all possible scattering events from a single site to calculate the disorder-averaged t -matrix, which is then related to the one-electron self energy as,

$$\hat{\Sigma}(\mathbf{k}, \omega) = n_{imp} \hat{T}_{\mathbf{k}, \mathbf{k}}(\omega), \quad (\text{A1})$$

where n_{imp} is the impurity concentration, and, for isotropic scatterers, $\hat{T}_{\mathbf{k}, \mathbf{k}}(\omega) = \hat{T}(\omega)$, and hence $\hat{\Sigma}(\omega)$, has no momentum dependence. For a multiband superconductor, scattering from impurities can occur within a given band with potential U_{ii} , or between the bands with potential U_{ij} , $i \neq j$. Fig. 12 shows the impurity averaged diagrams for the self energy Σ which occur up to third order for a two-band system. Any process which involves odd number of interband scatterings does not contribute to the self energy, because the Green’s function and self-energy in the translationally invariant disorder-averaged system are diagonal in band index.

The sum of all the diagrams involving a single impurity site can be expressed compactly as

$$\hat{T}_i = \frac{1}{1 - \hat{U}_i^{eff} \langle \hat{G}_i \rangle_k} \hat{U}_i^{eff} \quad (\text{A2})$$

where the effective impurity potential for i^{th} band is,

$$\hat{U}_i^{eff} = \hat{U}_{ii} + \hat{U}_{ij} \langle \hat{G}_j \rangle_k \hat{U}_{ji} \quad (\text{A3})$$

In a Nambu basis,

$$\hat{U}_{ij} = U_{ij} \tau_3 \quad (\text{A4})$$

$$\langle \hat{G}_i \rangle_k = g_{i,0} \tau_0 + g_{i,1} \tau_1 \quad (\text{A5})$$

Here $g_{i,\alpha}$ are the Nambu components of the momentum-integrated Green’s function. The first subscript i ($= 1, 2$) in $g_{i,\alpha}$ stands for the band and the second subscript α ($= 0, 1, 2, 3$) represents the Nambu channel.

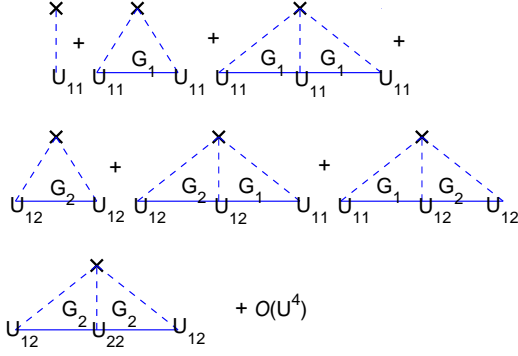


FIG. 12: These are the impurity averaged diagrams, which contribute to the self energy of the first band Green's function. Here the interband contribution comes through processes, which involve even number of interband scatterings. The diagrams also takes into account the order of inter and intraband scatterings. U_{ij} is the impurity potential strength, where i, j are the band indexes. $i = j$ denotes the intraband and $i \neq j$ denotes the interband potential strength. G_i is the bare Green's function.

The effective potential for the first band may be written

$$\hat{U}_{11}^{eff} = U_{11}\tau_3 + U_{12}^2\tau_3 \left[\hat{G}_2 \frac{1}{1 - \hat{U}_{22}\hat{G}_2} \right] \tau_3 \quad (\text{A6})$$

In the above equations, U_{11}, U_{22} are the intraband impurity potential strengths in band 1 and 2 respectively, while U_{12} is the interband impurity potential strength. The t -matrix for, e.g. the first band may now be written as

$$\hat{T}_1 = \frac{1}{1 - \hat{U}_{11}^{eff}\hat{G}_1} (\hat{U}_{11}^{eff}) \quad (\text{A7})$$

After some Pauli matrix algebra, we find that the self energy components in band and Nambu channels may be written as

$$\Sigma_{1,0} = \frac{n_{imp}}{\mathcal{D}} [U_{11}^2 g_{1,0} + U_{12}^2 g_{2,0} - g_{1,0}(U_{12}^2 - U_{11} U_{22})^2 (g_{2,0}^2 - g_{2,1}^2)] \quad (\text{A8})$$

$$\Sigma_{1,1} = -\frac{n_{imp}}{\mathcal{D}} [U_{11}^2 g_{1,1} + U_{12}^2 g_{2,1} - g_{1,0}(U_{12}^2 - U_{11} U_{22})^2 (g_{2,0}^2 - g_{2,1}^2)] \quad (\text{A9})$$

$$\Sigma_{2,\alpha} = \Sigma_{1,2 \rightarrow 2,1,\alpha} \quad (\text{A10})$$

$$\begin{aligned} \mathcal{D} = & 1 - 2 U_{12}^2 (g_{1,0} g_{2,0} - g_{1,1} g_{2,1}) \\ & + (U_{12}^2 - U_{11} U_{22})^2 (g_{1,0}^2 - g_{1,1}^2) (g_{2,0}^2 - g_{2,1}^2) \\ & - U_{22}^2 (g_{2,0}^2 - g_{2,1}^2) - U_{11}^2 (g_{1,0}^2 - g_{1,1}^2) \end{aligned} \quad (\text{A11})$$

Here again the first subscript in $\Sigma_{i,\alpha}$ represents the band index and the second subscript α denotes the Nambu channel.

APPENDIX B: SPECIAL CASES

1. Born limit of two band case

In the Born limit, we will keep the terms up to second order in " U_{ij} ", so the denominator becomes 1 and we get,

$$\Sigma_{1,0} = n_{imp} (U_{11}^2 g_{1,0} + U_{12}^2 g_{2,0}) \quad (\text{B1})$$

$$\Sigma_{1,1} = -n_{imp} (U_{11}^2 g_{1,1} + U_{12}^2 g_{2,2}) \quad (\text{B2})$$

$$\Sigma_{2,0} = n_{imp} (U_{22}^2 g_{2,0} + U_{12}^2 g_{1,0}) \quad (\text{B3})$$

$$\Sigma_{2,1} = -n_{imp} (U_{22}^2 g_{2,2} + U_{12}^2 g_{1,2}) \quad (\text{B4})$$

2. Strong potential limit

Due to the presence of an additional band, a new parameter comes into play in the unitary limit, the ratio of the interband scattering to the intraband scattering. This leads to three distinct cases in the large potential limit.

a. Strong potential limit I: $U_{11} = U_{22} > U_{12}$ In this case, intraband scattering dominates, and in the limit the self energies reduces to

$$\Sigma_{1,0} = -n_{imp} \frac{g_{1,0}}{(g_{1,0}^2 - g_{1,1}^2)} \quad (\text{B5})$$

$$\Sigma_{1,1} = n_{imp} \frac{g_{1,1}}{(g_{1,0}^2 - g_{1,1}^2)} \quad (\text{B6})$$

$$\Sigma_{2,0} = -n_{imp} \frac{g_{2,0}}{(g_{2,0}^2 - g_{2,1}^2)} \quad (\text{B7})$$

$$\Sigma_{2,1} = n_{imp} \frac{g_{2,1}}{(g_{2,0}^2 - g_{2,1}^2)} \quad (\text{B8})$$

It is clear that in this limit, states within a given band are broadened only by interband scattering processes.

b. Strong potential limit II: $U_{11} = U_{22} = U_{12}$. In this very special case, for strong potentials the self energies become

$$\Sigma_{1/2,0} = -n_{imp} \frac{g_{1,0} + g_{2,0}}{(g_{1,0} + g_{2,0})^2 - (g_{1,1} + g_{2,1})^2} \quad (\text{B9})$$

$$\Sigma_{1/2,1} = n_{imp} \frac{g_{1,1} + g_{2,1}}{(g_{1,0} + g_{2,0})^2 - (g_{1,1} + g_{2,1})^2} \quad (\text{B10})$$

$$(\text{B11})$$

In this case, both the bands have identical self energies. As discussed in the text, it corresponds to the presence of bound states at low energies in the s_{\pm} state, so we devote some attention to it.

- ¹ C.C. Tsuei and J.R. Kirtley, *Rev. Mod. Phys.* **72**, 969 (2000).
- ² Y. Kamihara, T. Watanabe, M. Hirano, and H. Hosono, *J. Am. Chem. Soc.* **130**, 3296 (2008).
- ³ K. Hashimoto, T. Shibauchi, T. Kato, K. Ikada, R. Okazaki, H. Shishido, M. Ishikado, H. Kito, A. Iyo, H. Eisaki, S. Shamoto, and Y. Matsuda, *Phys. Rev. Lett.* **102**, 017002 (2009).
- ⁴ C. Martin, M. E. Tillman, H. Kim, M. A. Tanatar, S. K. Kim, A. Kreyssig, R. T. Gordon, M. D. Vannette, S. Nandi, V. G. Kogan, S. L. Bud'ko, P. C. Canfield, A. I. Goldman, R. Prozorov, *Phys. Rev. Lett.* **102**, 247002 (2009).
- ⁵ K. Hashimoto, T. Shibauchi, S. Kasahara, K. Ikada, S. Tonegawa, T. Kato, R. Okazaki, C. J. van der Beek, M. Konczykowski, H. Takeya, K. Hirata, T. Terashima, Y. Matsuda, *Phys. Rev. Lett.* **102**, 207001 (2009).
- ⁶ R. T. Gordon, N. Ni, C. Martin, M. A. Tanatar, M. D. Vannette, H. Kim, G. Samolyuk, J. Schmalian, S. Nandi, A. Kreyssig, A. I. Goldman, J. Q. Yan, S. L. Bud'ko, P. C. Canfield, R. Prozorov, *Phys. Rev. Lett.* **102**, 127004 (2009).
- ⁷ R. T. Gordon, C. Martin, H. Kim, N. Ni, M. A. Tanatar, J. Schmalian, I. I. Mazin, S. L. Bud'ko, P. C. Canfield, R. Prozorov, *Phys. Rev. B* **79**, 100506 (2009).
- ⁸ J.D. Fletcher, A. Serafin, L. Malone, J. Analytis, J-H Chu, A.S. Erickson, I.R. Fisher, A. Carrington, *Phys. Rev. Lett.* **102**, 147001 (2009).
- ⁹ Lin Zhao, Haiyun Liu, Wentao Zhang, Jianqiao Meng, Xiaowen Jia, Guodong Liu, Xiaoli Dong, G. F. Chen, J. L. Luo, N. L. Wang, Guiling Wang, Yong Zhou, Yong Zhu, Xiaoyang Wang, Zhongxian Zhao, Zuyan Xu, Chuangtian Chen, X. J. Zhou, *Chin. Phys. Lett.* **25**, 4402 (2008).
- ¹⁰ H. Ding, P. Richard, K. Nakayama, T. Sugawara, T. Arakane, Y. Sekiba, A. Takayama, S. Souma, T. Sato, T. Takahashi, Z. Wang, X. Dai, Z. Fang, G.F. Chen, J.L. Luo, N.L. Wang, *Europhys. Lett.* **83**, 47001 (2008).
- ¹¹ T. Kondo, A.F. Santander-Syro, O. Copie, C. Liu, M.E. Tillman, E.D. Mun, J. Schmalian, S.L. Bud'ko, M.A. Tanatar, P.C. Canfield, A. Kaminski, *Phys. Rev. Lett.* **101**, 147003 (2008).
- ¹² D.V. Evtushinsky, D.S. Inosov, V.B. Zabolotnyy, A. Koitzsch, M. Knupfer, B. Buchner, G.L. Sun, V. Hinkov, A.V. Boris, C.T. Lin, B. Keimer, A. Varykhalov, A.A. Kordiyuk, S.V. Borisenko, *Phys. Rev. B* **79**, 054517 (2009).
- ¹³ K. Nakayama, T. Sato, P. Richard, Y.-M. Xu, Y. Sekiba, S. Souma, G. F. Chen, J. L. Luo, N. L. Wang, H. Ding, T. Takahashi, *Euro. Phys. Lett.* **85**, 67002 (2009).
- ¹⁴ L. Wray, D. Qian, D. Hsieh, Y. Xia, L. Li, J.G. Checkelsky, A. Pasupathy, K.K. Gomes, C.V. Parker, A.V. Fedorov, G.F. Chen, J.L. Luo, A. Yazdani, N.P. Ong, N.L. Wang, M.Z. Hasan, *Phys. Rev. B* **78**, 184508 (2008).
- ¹⁵ R. Klingeler, N. Leps, I. Hellmann, A. Popa, C. Hess, A. Kondrat, J. Hamann-Borrero, G. Behr, V. Kataev, and B. Buechner, *arXiv:0808.0708*.
- ¹⁶ K. Matano, Z. A. Ren, X. L. Dong, L. L. Sun, Z. X. Zhao and Guo-qing Zheng, *Europhysics Letters* **83**, 57001 (2008).
- ¹⁷ H.-J. Grafe, D. Paar, G. Lang, N.J. Curro, G. Behr, J. Werner, J. Hamann-Borrero, C. Hess, N. Leps, R. Klingeler, and B. Buchner, *Phys. Rev. Lett.* **101**, 047003 (2008).
- ¹⁸ K. Ahilan, F.L. Ning, T. Imai, A.S. Sefat, R. Jin, M.A. McGuire, B.C. Sales, D. Mandrus, *Phys. Rev. B* **78**, 100501(R) (2008).
- ¹⁹ T.Y. Nakai et al., *J. Phys. Soc. Jpn.* **77**, 073701 (2008).
- ²⁰ M. Yashima, H. Nishimura, H. Mukuda, Y. Kitaoka, K. Miyazawa, P. M. Shirage, K. Kiho, H. Kito, H. Eisaki, and A. Iyo, *arXiv:0905.1896* (unpublished).
- ²¹ L. Shan, Y. Wang, X. Zhu, G. Mu, L. Fang, C. Ren and H.-H. Wen, *Europhys. Lett.* **83**, 57004 (2008).
- ²² T.Y. Chien, Z. Tesanovic, R.H. Liu, X.H. Chen, and C.L. Chien, *Nature* **453**, 1224 (2008).
- ²³ D. Daghero, M. Tortello, R.S. Gonnelli, V.A. Stepanov, N.D. Zhigadlo and J. Karpinski, *Journal of superconductivity and novel magnetism*, **22**,553 (2009).
- ²⁴ R.S. Gonnelli, D. Daghero, M. Tortello, G.A. Ummarino, V.A. Stepanov, J.S. Kim and R.K. Kremer, *Phys. Rev. B* **79**, 184526 (2009).
- ²⁵ Y. Matsuda, K. Izawa, and I. Vekhter, *J. Phys.: Cond. Mat.* **18**, R705-R752 (2006).
- ²⁶ H. Shakeripour, C. Petrovic, Louis Taillefer, *New Journal of Physics* **11**, 055065 (2009).
- ²⁷ J. G. Checkelsky, Lu Li, G. F. Chen, J. L. Luo, N. L. Wang and N. P. Ong, *arXiv:0811.4668*.
- ²⁸ X. G. Luo, M. A. Tanatar, J.-Ph. Reid, H. Shakeripour, N. Doiron-Leyraud, N. Ni, S. L. Budko, P. C. Canfield, Huiqian Luo, Zhaosheng Wang, Hai-Hu Wen, Ruslan Prozorov, and Louis Taillefer, *arXiv:0904.4049*.
- ²⁹ L. Ding, J. K. Dong, S. Y. Zhou, T. Y. Guan, X. Qiu, C. Zhang, L. J. Li, X. Lin, G. H. Cao, Z. A. Xu, and S. Y. Li, *arXiv:0906.0138*.
- ³⁰ Y. Machida, K. Tomokuni, T. Isono, K. Izawa, Y. Nakajima, and T. Tamegai, *arXiv:0906.0508*.
- ³¹ M. Yamashita, N. Nakata, Y. Senshu, S. Tonegawa, K. Ikada, K. Hashimoto, H. Sugawara, T. Shibauchi, and Y. Matsuda, *arXiv:0906.0622*.
- ³² Note that there is substantial disagreement in the low-temperature behavior of Co-doped samples between Refs. 30 and 37.
- ³³ G. Preosti and P. Muzikar, *Phys. Rev. B* **54**, 3489 (1996).
- ³⁴ A.A. Golubov and I.I. Mazin, *Phys. Rev. B* **55**, 15146 (1997).
- ³⁵ Y. Senga and H. Kontani, *J. Phys. Soc. Jpn.* **77**, 113710 (2008); *New J. Phys.* **11**, 035005(2009).
- ³⁶ Y. Bang, H.-Y. Choi, and H. Won, *Phys. Rev. B* **79**, 054529 (2009).
- ³⁷ M. A. Tanatar, J. P. Reid, H. Shakeripour, X. G. Luo, N. Doiron-Leyraud, N. Ni, S. L. Bud'ko, P. C. Canfield, R. Prozorov, Louis Taillefer, *arXiv:0907.1276* (unpublished).
- ³⁸ V. Mishra, G. Boyd, S. Graser, T. Maier, P.J. Hirschfeld, and D.J. Scalapino, *Phys. Rev. B* **79**, 094512 (2009).
- ³⁹ K. Kuroki, S. Onari, R. Arita, H. Usui, Y. Tanaka, H. Kontani and H. Aoki, *Phys. Rev. Lett.* **101**, 087004 (2008).
- ⁴⁰ F. Wang, H. Zhai, Y. Ran, A. Vishwanath and D.-H. Lee, *Phys. Rev. Lett.* **102**, 047005 (2009).
- ⁴¹ S. Graser, T. A. Maier, P. J. Hirschfeld, and D. J. Scalapino, *New J. Phys.* **11**, 025016 (2009).
- ⁴² T. Maier, S. Graser, P.J. Hirschfeld, and D.J. Scalapino, *Phys. Rev. B* **79**, 224510 (2009).
- ⁴³ A.V. Chubukov, M.G. Vavilov, A.B. Vorontsov, *arXiv:0903.5547*.

- ⁴⁴ R. Thomale, C. Platt, J. Hu, C. Honerkamp, B. A. Bernevig arXiv:0906.4475.
- ⁴⁵ I. I. Mazin, D. J. Singh, M. D. Johannes, and M. H. Du, Phys. Rev. Lett. **101**, 057003 (2008).
- ⁴⁶ A. V. Chubukov, D. Efremov, and I. Eremin, Phys. Rev. B **78**, 134512 (2008).
- ⁴⁷ V. Ambegaokar and A. Griffin, Phys. Rev. **137**, A1151 - A1167 (1965).
- ⁴⁸ C. Cao, P. J. Hirschfeld, H.-P. Cheng, Phys. Rev. B **77**, 220506(R) (2008).
- ⁴⁹ P. A. Lee, Phys. Rev. Lett. **71**, 1887 (1993).
- ⁵⁰ M. Graf J. A. Sauls, Phys. Rev. Lett. **53**, 15147 (1996).
- ⁵¹ M. Norman and P. J. Hirschfeld, Phys. Rev. B **53**, 5706 (1996).
- ⁵² M. T. Beal-Monod and K. Maki, Physica C **265**, 309 (1996).
- ⁵³ L. S. Borkowski and P. J. Hirschfeld, Phys. Rev. B **49**, 15404 (1994).
- ⁵⁴ R. Fehrenbacher and M. R. Norman, Phys. Rev. B **50**, 3495 (1994).
- ⁵⁵ A. B. Vorontsov, M. G. Vavilov, and A. V. Chubukov, Phys. Rev. B **79**, 140507 (2009).
- ⁵⁶ D. Parker, O. V. Dolgov, M. M. Korshunov, A. A. Golubov, and I. I. Mazin, Phys. Rev. B **78**, 134524 (2008).
- ⁵⁷ A. V. Chubukov, D. Efremov, and I. Eremin, Phys. Rev. B **78**, 134512 (2008).
- ⁵⁸ D. Markowitz and L. P. Kadanoff, Phys. Rev. **131**, 563 (1963).
- ⁵⁹ A. A. Abrikosov and L. P. Gor'kov, Zh. Eksp. Teor. Fiz **39**, 1781(1960) [Sov. Phys. JETP **12**, 1243(1961)].
- ⁶⁰ L. P. Gorkov and P. A. Kalugin, Pisma Zh. Eksp. Teor. Fiz. **41**, 208 (1985) [JETP Lett. **41**, 263 (1985)].
- ⁶¹ K. Ueda and M. Rice, 1985, in *Theory of Heavy Fermions and Valence Fluctuations*, edited by T. Kasuya and T. Saso (Springer-Verlag, Berlin), p. 216.
- ⁶² M. Sigrist and K. Ueda, Rev. Mod. Phys. **63**, 239 (1991).
- ⁶³ S. Skalski, O. Betbeder-Matibet, and P. R. Weiss, Phys. Rev. **136**, A1500 (1964).
- ⁶⁴ P. J. Hirschfeld, P. Wölfle and D. Einzel, Phys. Rev. B **37**, 83 (1988).
- ⁶⁵ We have averaged the xx and yy components to simulate the ferropnictide with order parameters on β_1 and β_2 sheets rotated by $\pi/2$ in local coordinates with respect to one another.
- ⁶⁶ The approximate factor of 2 difference between the kink temperature and the antinodal order parameter energy energy arises from the width of the thermal quasiparticle distribution.
- ⁶⁷ F. Gross, B. S. Chandrasekhar, D. Einzel, P. J. Hirschfeld, K. Andres, H. R. Ott, J. Beuers, Z. Fisk and J. L. Smith, Z. Physik B **64**, 175 (1986).
- ⁶⁸ I. Koztin and A. J. Leggett, Phys. Rev. Lett. **79**, 135 (1997).
- ⁶⁹ Y. Kamihara, et al. J. Amer. Chem. Soc. **128**, 10012 (2006).
- ⁷⁰ A. I. Coldea et al., Phys. Rev. Lett. **101**, 216402 (2008).
- ⁷¹ P. J. Hirschfeld and N. Goldenfeld, Phys. Rev. B. **48**, 4219(1993).
- ⁷² L. S. Borkowski, P. J. Hirschfeld, and W. O. Putikka, Phys. Rev. B **52**, 3856 (1995).
- ⁷³ R. Movshovich, M. Jaime, J. D. Thompson, C. Petrovic, Z. Fisk, P. G. Pagliuso, and J. L. Sarrao, Phys. Rev. Lett. **86**, 5152 (2001).
- ⁷⁴ M. Sutherland, D. G. Hawthorn, R. W. Hill, F. Ronning, S. Wakimoto, H. Zhang, C. Proust, Etienne Boaknin, C. Lupien, Louis Taillefer, Ruixing Liang, D. A. Bonn, W. N. Hardy, Robert Gagnon, N. E. Hussey, T. Kimura, M. Nohara, and H. Takagi, Phys. Rev. B **67**, 174520 (2003).
- ⁷⁵ E. Boaknin, M. A. Tanatar, Johnpierre Paglione, D. Hawthorn, F. Ronning, R. W. Hill, M. Sutherland, L. Taillefer, J. Sonier, S. M. Hayden, and J. W. Brill, Phys. Rev. Lett. **90**, 117003 (2003).
- ⁷⁶ Louis Taillefer, Benoit Lussier, Robert Gagnon, Kamran Behnia, and Herv Aubin, Phys. Rev. Lett. **79**, 483 (1997).
- ⁷⁷ G. E. Volovik, JETP Letters **58**, 469 (1993).
- ⁷⁸ C. Kübert and P. J. Hirschfeld, Solid State Commun. **105**, 459 (1998).
- ⁷⁹ I. Vekhter, P. J. Hirschfeld, and E. J. Nicol, Phys. Rev. B **64**, 064513 (2001).
- ⁸⁰ C. Kübert and P. J. Hirschfeld, Phys. Rev. Lett. **80**, 4963 (1998).
- ⁸¹ M. Franz, Phys. Rev. Lett. **82**, 1760 (1999).
- ⁸² I. Vekhter and P. J. Hirschfeld, Physica C **341-348**, 1947 (2000).
- ⁸³ I. Vekhter, L. N. Bulaevskii, A. E. Koshelev, and M. P. Maley, Phys. Rev. Lett. **84**, 1296 (2000).
- ⁸⁴ U. Brandt, W. Pesch, and L. Tewordt, Z. Phys. **201**, 209 (1967).
- ⁸⁵ W. Pesch, Z. Phys. B **21**, 263 (1975).
- ⁸⁶ A. Houghton and K. Maki, Phys. Rev. B **4**, 843 (1971).
- ⁸⁷ P. Klimesch and W. Pesch, J. Low Temp. Phys. **32**, 869 (1978).
- ⁸⁸ E. H. Brandt, J. Low Temp. Phys. **24**, 409 (1976).
- ⁸⁹ I. Vekhter and A. Houghton, Phys. Rev. Lett. **83**, 4626 (1999).
- ⁹⁰ H. Kusunose, Phys. Rev. B **70**, 054509 (2004).
- ⁹¹ A. B. Vorontsov and I. Vekhter, Phys. Rev. Lett. **96**, 237001 (2006).
- ⁹² A. B. Vorontsov and I. Vekhter, Phys. Rev. B **75**, 224501 (2007).
- ⁹³ A. B. Vorontsov and I. Vekhter, Phys. Rev. B **75**, 224502 (2007).
- ⁹⁴ T. Dahm, S. Graser, C. Iniotakis, and N. Schopohl, Phys. Rev. B **66**, 144515 (2002).
- ⁹⁵ G. R. Boyd, P. J. Hirschfeld, I. Vekhter, and A. B. Vorontsov, Phys. Rev. B **79**, 064525 (2009).